Extended Abstracts of the 2007 International Conference on Solid State Devices and Materials, Tsukuba, 2007, pp. 92-93

D-2-4

Performance of Tense Thin Film Torsion Bar for Large-Rotation and Low-Voltage Driving of Micromirror

Minoru Sasaki[1], Shinya Yuki[2], Kazuhiro Hane[2]
[1]Toyota Technological Institute, Dept. of Advanced Science and Technology
Hisakata 2-12-1, Tenpaku-ku, Nagoya 468-8511, Japan
Phone: +81-52-809-1840 E-mail: mnr-sasaki@toyota-ti.ac.jp
[2]Tohoku University, Dept. of Nanomechanics
Aza-Aoba 6-6-01 Aramaki, Aoba-ku, Sendai 980-8579, Japan

1. Introduction

The electrostatic actuator is preferred in the mocromirror due to the little power consumption. The limitation of the electrostatic driving is the difficulty for realizing the large rotation angle with the low voltage driving. The goal will be working under the power source of the existent system (e.g., 5, 12, 24 V). Limited devices have succeeded to satisfy this requirement. Hah et al. reported the micromirror fabricated by the surface micromachining [1]. The rotation angle is 5.9° at 6 V. The spring constant for the mirror rotation should be minimized maintaining the rigidity in other motions. The serpentine spring helps the design, but does not completely solve the problem [2]. In many cases, the pull-in instability occurs at the weakest direction (not rotation) and limits the rotation angle.

We have introduced the thin film torsion bar for realizing low-voltage driving of the mirror [3]. The tension is included in the torsion bar for increasing the rigidity against the unwanted mirror motion. In this study, the performance of the tense thin film torsion bar is investigated.

2. Principle

When the torsion bar has the rectangular cross-section, the torsional spring constant $k_?$ is expressed as follows.

$$k_q \approx \frac{Gwt^3}{3l}\left(1-\frac{192}{p^5}\frac{t}{w}\tanh\frac{pw}{2t}\right) \tag{1}$$

G is the shear modulus. l is the length of torsion bar. w and t are width or thickness, supposing the relation of $w>t$. When thin films are considered, t is the thickness. The factor t^3 shows that decreasing t is effective for decreasing $k_?$. The estimated value is 1.4x10^{-11} Nm/rad by setting G, l, w, and t as 80 GPa, 200, 4, and 0.3 µm, respectively.

Figure 1 shows the schematic drawing. The tension works against the vertical displacement of the mirror. The tensile stress s_0 inside SiN film can be 760 MPa [4], and the tension s_0wt is 910 mN for 4x0.3 µm^2 cross-section. This value is significantly large compared to the driving force of ~7 nN in our design. Since the thin film torsion bar is softest in the vertical direction, the vertical spring constant k_z becomes important. k_z is expressed as follows.

$$k_z \approx \frac{1}{\sum_{n=1,odd}^{\infty}\frac{1}{l}\frac{2}{\frac{Ewt^3}{12}k_n^{\ 4}+s_0wtk_n^{\ 2}}}, \qquad k_n=\frac{np}{l} \quad (n=1,3,5\cdots) \tag{2}$$

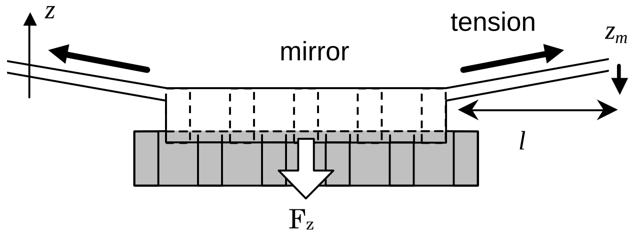

Fig. 1. Effect of tension in the torsion bar for suppressing the vertical displacement.

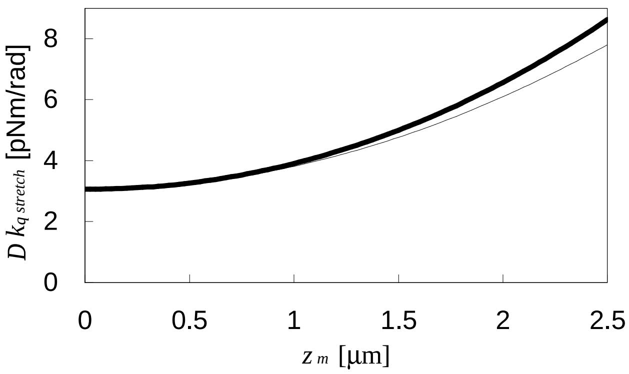

Fig. 2. Curves calculated from eq. (3). The thick and thin black curves are the sum of all terms and the contribution of proportional to the stress s_0, respectively.

The elasticity E is set to 290 GPa. When s_0 is 0 and 760 MPa, k_z is 0.016 and 19 N/m, respectively. The increased spring constant suppresses the vertical displacement. The increase of the torsional spring constant $Dk_{q\ \mathrm{stretch}}$ generated by the beam stretching can be estimated as follows.

$$Dk_{q\ stretch} \approx \frac{wt}{l}\left\{s_0\left(\frac{t^2}{24}+\frac{w^2}{24}+\frac{z_m^{\ 2}}{6}\right)+\frac{Ez_m^{\ 2}}{l^2}\left(\frac{t^2}{24}+\frac{w^2}{8}+\frac{z_m^{\ 2}}{6}\right)\right\}$$
$$+q^2E\frac{wt}{l^3}\left\{\frac{t^4}{160}+\frac{t^2w^2}{144}+\frac{w^4}{160}+z_m^{\ 2}\left(\frac{t^2}{12}+\frac{w^2}{36}+\frac{z_m^{\ 2}}{10}\right)\right\} \tag{3}$$

z_m is the vertical shift occurred with the mirror rotation (measured to be a few µm). The terms wts_0/l ($t^2/24+w^2/24+z_m^2/6$) corresponds to stretching against the tension. The other terms correspond to the elastic stretching showing the linear dependence on the elasticity E. These terms are minor. Evaluate some values by setting z_m=0 for clearing the main feature. The dominant part relating to stretching against the stress s_0 has the value of 3.1x10^{-12} Nm/rad. This is 22% of the spring constant estimated from eq.(1). Without the vertical shift z_m, the tension is fundamentally per-

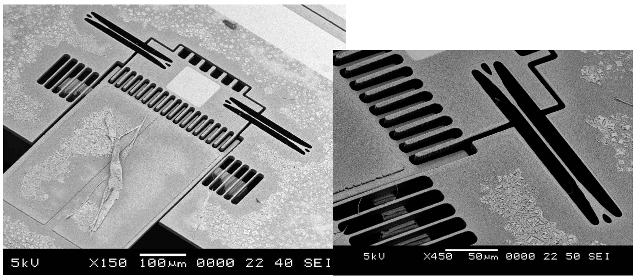

Fig. 3. Fabricated micromirror.

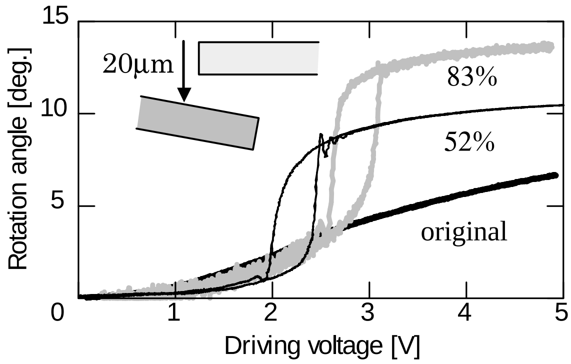

Fig. 4. Mirror rotation angle as a function of the driving voltage Thick black, thick gray, thin black curves correspond to the tension having the original, 83%, and 52% values, respectively.

pendicular to the rotational displacement of the material inside the torsion bar.

Figure 2 shows the curves calculated based on eq.(3). The thick and thin black curves show the all terms and the contribution of wts_0/l ($t^2/24+w^2/24+z_m^2/6$), respectively. 5^{o} mirror rotation with z_m=2.5 μm is supposed keeping the linear relation. Supposing $t<<w$, the contribution of z_m in terms wts_0/l ($t^2/24+w^2/24+z_m^2/6$) increases significantly under the condition of $z_m>w/2$. With z_m generated with the electrostatic force, k_q increases with the mirror rotation.

3. Results and Discussion

Figure 3 shows a fabricated micromirror. The magnified image shows the torsion bar and the vertical comb. The designed dimension of the torsion bar is 200x4x0.3 μm^3.

The relation between the mirror rotation angle and the tension inside the torsion bar is investigated. The tension is decreased by the compress stress added by the implantation of boron ion. The values of the tensile stress are monitored using the strain gauge [5]. The estimated stress and the original tension are 780 MPa and 940 mN, respectively.

Figure 4 shows a series of the mirror rotation angle as the function of the driving voltage showing the round trip motions. The comb-to-comb distance is 20 μm having the vertical gap of 10 μm as shown in the inset. The electrode condition becomes similar to that of the parallel plate. The saturated rotation angle of 83% tension is larger than that of 52% tension. The curves with decreased tension show the pull-in phenomenon. The pull-in voltage (3.0 V) of 83% tension is larger than that (2.4 V) of 52% tension. The

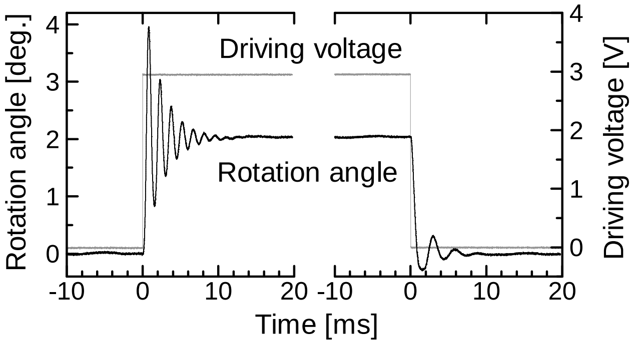

Fig. 5. Step response of the micromirror. The driving voltage is 3 V. The device has 8.2 μm comb-to-comb height difference between combs and 100% tension in the torsion bar.

stably obtainable rotation angle before the pull-in is 7 and 3.5^{o} for 83 and 52% tensions, respectively. For 52% tension, the rotation angle of 3.5^{o} is nearly 1/3 of the saturated angle of 10.4^{o}. 100% tension keeps the mirror stable up to 7^{o}. The curve of 100% tension is rather linear. This is advantageous for controlling the rotation angle. The hysteresis in the round trip motion is small with 100% tension. At the voltage of ~2 V, the torsion bar with 100% tension shows the largest rotation angle. The electrostatic force is efficiently converted to the mirror rotation not to the vertical shift.

Figure 5 shows 3 V step response. The comb-to-comb distance is 8.2 μm. The tension is original 100%. The overshoot oscillation is observed. The ringing periods are 1.5 ms (670 Hz) and 2.8 ms (360 Hz) for the rise up and the fall down steps, respectively. The increased ringing frequency at the rise up step is explained by the hard-spring effect. This increasing ratio is significantly large compared to the case using usual torsion bar. Filhol et al. reported ~0.63% increase of the resonant frequency when the mirror rotates by 50^{o}. The torsion bar has dimensions of 400x8.5x20 μm^3 without tension [6]. These features agree with eq.(3). The non-linear terms proportional to q^2 have small values compared to other terms. The curve of the rotation angle with 100% tension in Fig. 4 is rather linear. The hard-spring effect is considered to cancel the non-linearity of the electrostatic actuator to some extent.

References

[1] D. Hah, S. T. Huang, J. Tsai, H. Toshiyoshi, M. C. Wu, J. Microelectromechanical Systems, Vol. 13, 279-289, 2004.
[2] G. Barillaro, A. Molfese, A. Nannini, F. Pieri, J. Micromech. Microeng. Vol. 15, 736-746, 2005.
[3] M. Sasaki, S. Yuki, K. Hane, IEEE Photonics Technology Letters, Vol. 18, 1573-1575, 2006.
[4] M. Sekimoto, H. Yoshihara, T. Ohkubo, Y. Saitoh, Japanese J. Applied Physics, Vol. 20, L669-L672, 1981.
[5] L. Lin, A. P. Pisano, R. T. Howe, J. Microelectromechanical Systems, Vol. 6, pp.313-321, December, 1997.
[6] F. Filhol, E. Defay, C. Divoux, C. Zinck, M.-T. Delaye, Sensors and Actuators, Vol. A123-24, 483-489, 2005.